

See discussions, stats, and author profiles for this publication at: <https://www.researchgate.net/publication/258827092>

MXene: A New Family of Promising Hydrogen Storage Medium

ARTICLE *in* THE JOURNAL OF PHYSICAL CHEMISTRY A · NOVEMBER 2013

Impact Factor: 2.69 · DOI: 10.1021/jp409585v · Source: PubMed

CITATIONS

32

READS

297

8 AUTHORS, INCLUDING:



[Qianku Hu](#)

Henan Polytechnic University

26 PUBLICATIONS 195 CITATIONS

[SEE PROFILE](#)



[Dandan Sun](#)

Henan Polytechnic University

9 PUBLICATIONS 75 CITATIONS

[SEE PROFILE](#)



[Aiguo Zhou](#)

Henan Polytechnic University

45 PUBLICATIONS 707 CITATIONS

[SEE PROFILE](#)

MXene: A New Family of Promising Hydrogen Storage Medium

Qianku Hu,^{*,†,‡} Dandan Sun,[†] Qinghua Wu,[†] Haiyan Wang,[†] Libo Wang,[†] Baozhong Liu,[†] Aiguo Zhou,^{*,†} and Julong He[§]

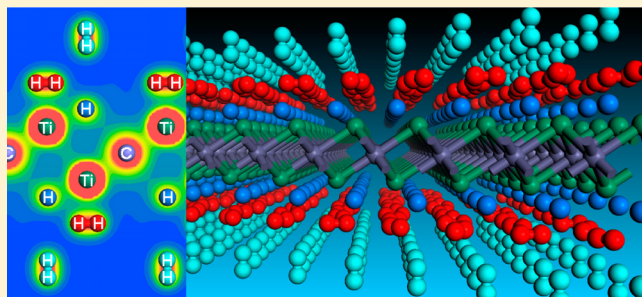
[†]School of Material Science and Engineering, Henan Polytechnic University, 454000 Jiaozuo, P. R. China

[‡]Department of Geosciences, Stony Brook University, 11794 Stony Brook, New York, United States

[§]State Key Laboratory of Metastable Materials Science and Technology, Yanshan University, 066004 Qinhuangdao, P. R. China

Web-Enhanced Feature Supporting Information

ABSTRACT: Searching for reversible hydrogen storage materials operated under ambient conditions is a big challenge for material scientists and chemists. In this work, using density functional calculations, we systematically investigated the hydrogen storage properties of the two-dimensional (2D) Ti₂C phase, which is a representative of the recently synthesized MXene materials (*ACS Nano* 2012, 6, 1322). As a constituent element of 2D Ti₂C phase, the Ti atoms are fastened tightly by the strong Ti–C covalent bonds, and thus the long-standing clustering problem of transition metal does not exist. Combining with the calculated binding energy of 0.272 eV, ab initio molecular dynamic simulations confirmed the hydrogen molecules (3.4 wt % hydrogen storage capacity) bound by Kubas-type interaction can be adsorbed and released reversibly under ambient conditions. Meanwhile, the hydrogen storage properties of the other two MXene phases (Sc₂C and V₂C) were also evaluated, and the results were similar to those of Ti₂C. Therefore, the MXene family including more than 20 members was expected to be a good candidate for reversible hydrogen storage materials under ambient conditions.



INTRODUCTION

Nowadays hydrogen storage and transport remain a great challenge for its vehicle applications.^{1,2} Storing hydrogen in solid materials is more practical, safe, and economic than that in gaseous or liquid phases.^{1–4} According to the interaction nature between hydrogen and host materials, solid-state storage materials can be classified into two categories: chemisorption of dissociated hydrogen atoms and physisorption of intact hydrogen molecules. Either approach has its own disadvantages. For chemisorption, strong bonding (40–80 kJ/mol)^{5,6} between hydrogen atoms and host materials (mainly metal hydrides or complex chemical hydrides) makes it difficult to release hydrogen at moderate temperatures. For physisorption, an ideal sorbent material should possess two fundamental properties: high specific surface area and suitable binding energy (20–30 kJ/mol, corresponding to ~0.2–0.3 eV)^{5,7} with hydrogen molecules. The sorption-based storage materials studied now mainly comprise carbon-base materials^{8–12} (including nanotubes, fullerenes, graphene, and nanoporous carbon), metal–organic frameworks (MOFs),^{13,14} and covalent organic frameworks (COFs).¹⁵ Almost all these materials meet the first requirement. For example, both sides of graphene can be utilized to store hydrogen,^{10,11} and the highest Brunauer–Emmett–Teller surface area of MOF tested to date reach about 7000 m²/g.¹⁶ However, the weak binding strength of hydrogen (4–10 kJ/mol, physisorption mostly by van der Waals forces)⁵ is the largest obstacle for the practical application of these

materials.¹⁷ At present these sorption-based hydrogen storage materials can only operate around liquid nitrogen temperature.

Metal decorations were employed to increase the binding energy of hydrogen on sorption-based materials. A great deal of theoretical calculation has been conducted to investigate the effects of metal decorations (including alkali, alkaline earth, and transition metals).^{18–28} The transition metal results are more exciting. Via Kubas-type interaction,²⁹ the binding energies of hydrogen with the transition metals lies between strong chemisorption and weak physisorption and comes into a desirable range. However, because of their large cohesive energies, transition-metal adatoms have a tendency of aggregating into clusters,²⁰ which would significantly reduce the hydrogen storage capacity.³⁰ Some calculations show that boron-doping or vacancy defects on carbon adsorbents may prevent the clustering behavior of metal adatoms.^{27,31,32} However, it is very difficult to fabricate such metal-well-dispersed carbon adsorbents with boron-doping or vacancy defects. Despite these problems, the Kubas-type hydrogen storage mode is still a promising direction. A material, with lightweight, high specific surface area, no metal-clustering behavior and exhibiting Kubas interactions to store hydrogen, is very hopeful to meet the gravimetric storage capacity target

Received: September 25, 2013

Revised: November 20, 2013

Published: November 21, 2013

(5.5 wt % by 2015)³³ set by the U.S. DOE. However, the discovery and synthesis of such material is of great challenge.

Recently, a new family of graphene-like 2D materials, named as MXene, was prepared by exfoliating the counterpart MAX phases in hydrofluoric acid.^{34,35} MAX phases are a large family (>60 members) of layered ternary transition-metal carbides or nitrides with a chemical formula $M_{n+1}AX_n$ ($n = 1, 2$, or 3), where M is a transition metal, A is an A-group element (mostly IIIA or IVA group), and X is C and/or N.^{36,37} To date, the as-synthesized MXene phases include Ti_2C , Ti_3C_2 , Ta_4C_3 , $(Ti_{0.5}Nb_{0.5})_2C$, $(V_{0.5}Cr_{0.5})_3C_2$, and Ti_3CN .^{34,35} For a new material, it is very important scientifically and technically to explore its basic properties and potential applications. Good electrical conductivities of bare MXenes were predicted theoretically and can be tuned by termination/functionalization with different groups.^{34,35,38–40} The electrochemical intercalation behaviors of Li ions in MXene structures were also investigated experimentally and theoretically, which prove MXene phases are very promising as anode materials of Li-ion battery.^{41–44}

In this paper, we investigated the possibility of employing MXene phases as hydrogen storage media by first-principles calculations. We chose Ti_2C as a representative of MXenes on the basis of the following reasons: (i) Titanium is a commonly used decoration element and has been proved to be effective for hydrogen storage in carbon-based materials. (ii) The 2D Ti_2C phase has already been synthesized (though with fluorine (F) and/or hydroxyl (OH) termination).³⁵ (iii) Except for Sc_2C , Ti_2C possesses the highest surface area per weight among all possible MXene phases, and thus it is expected to have high gravimetric hydrogen storage capacities. Figure 1 gives the

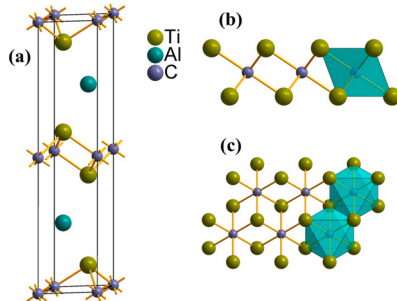


Figure 1. (a) Crystal structure of bulk Ti_2AlC . The black solid line labels out the unit cell. (b) Side views and (c) top views of 2D Ti_2C structure. Two Ti_2C octahedrons were labeled out by green color.

crystal structures of bulk Ti_2AlC and 2D Ti_2C . In the layered Ti_2AlC structure, Ti-Al bond is relatively weaker than Ti-C bond. Consequently, the layers of Al atoms can be selectively etched by hydrofluoric acid, which results in the formation of the 2D Ti_2C sheets.³⁵ The 2D Ti_2C structure is composed of sharing-edge Ti_6C octahedrons, in which, C atoms occupy the octahedral interstitial sites between near-close-packed Ti atoms. One Ti_2C sheet can be simply considered as one graphene sheet coated with a Ti atoms sheet on each side. These Ti atoms indeed are constituent elements of Ti_2C , and thus the problem of aggregation of Ti atoms can be avoided. With the cleavage of Ti-Al bond, all Ti atoms of Ti_2C lie in an unsaturated coordination state, which is an indispensable condition for metal atoms to exhibit the Kubas interactions.^{5,45} On the basis of aforementioned reasons, we think 2D Ti_2C (even most MXene phases) is very likely to be a reversible and

high-gravimetric-capacity hydrogen storage material operated under ambient conditions. The purpose of the calculations in this paper is to confirm this speculation.

THEORETICAL METHODS

Our first-principles total energy pseudopotential calculations were performed using the density functional theory (DFT) as implemented in CASTEP code.⁴⁶ The exchange and correlation energy is described by the local density approximation (LDA) functional. Vanderbilt ultrasoft pseudopotentials were employed within a plane wave basis set with the cutoff energy of 480 eV. The numerical integration of the Brillouin zone was performed using $6 \times 6 \times 2$ (unit cell) and $2 \times 2 \times 1$ (supercell) Monkhorst-Pack (MP) k -point sampling. Both structural parameters and atomic positions with no constraints were fully relaxed using the BFGS minimization method until the convergence tolerance (energy $< 5.0 \times 10^{-6}$ eV, force < 0.01 eV/ \AA , stress < 0.02 GPa and displacement $< 5.0 \times 10^{-4}$ \AA) was reached.

The binding energy (E_b) of H_2 with the Ti_2C host material was calculated according to the following equation:

$$E_b = (E_{\text{host}} + nE_{H_2} - E_{\text{host}+nH_2})/n$$

where E_{host} is the total energy of the host structure (bare Ti_2C structure or already adsorbed with some H_2 or H), E_{H_2} is the total energy of a free H_2 , $E_{\text{host}+nH_2}$ is the total energy of the host structure adsorbed with new hydrogen molecules, and n is the number of new adsorbed hydrogen molecules. The binding energy of H atom to the surface of Ti_2C was also calculated like this.

RESULTS AND DISCUSSION

Ti_2C Model. The 2D Ti_2C structure was constructed by removing the Al element from the parent Ti_2AlC structure. Thereafter, a vacuum space with a thickness of 20 \AA was inserted between the neighboring slabs to avoid artificial interactions between them. The optimized lattice constant a for the Ti_2C model is 3.002 \AA , which is in good agreement with the other result of 3.007 \AA .³⁸

A Ti_2C 3×3 periodic supercell (containing nine carbon and eighteen titanium atoms, shown in Figure 2a) was used as the host material. To investigate the hydrogen adsorption, it is important to first find the favorable adsorption sites. On Ti_2C surfaces, there exist three types of high-symmetry sites: top site over a Ti atom at the top surface; hollow_1 site above the center of three Ti atoms at the top surface, under which there exists one Ti atom at the bottom surface; and hollow_2 site above the center of three Ti atoms at the top surface, under which there exists one C atom at the bottom surface.

Hydrogen at Ti_2C 3×3 Supercell. We first studied the adsorption of a single hydrogen molecule on the Ti_2C 3×3 supercell. A H_2 molecule was put parallel or perpendicularly above the three adsorption sites respectively, and thus six models were constructed, which are shown in Figure 2a. After geometry optimization, the H_2 initially locating parallel above the three sites and perpendicularly above the hollow_2 site is thermally unstable and dissociates into two H atoms. Nearly all dissociated H atoms occupy the hollow_1 site. The calculations (Supporting Information) for one hydrogen atom locating above the top, hollow_1 and hollow_2 sites, respectively, show that the hollow_1 site is the most stable one. Thus it can be

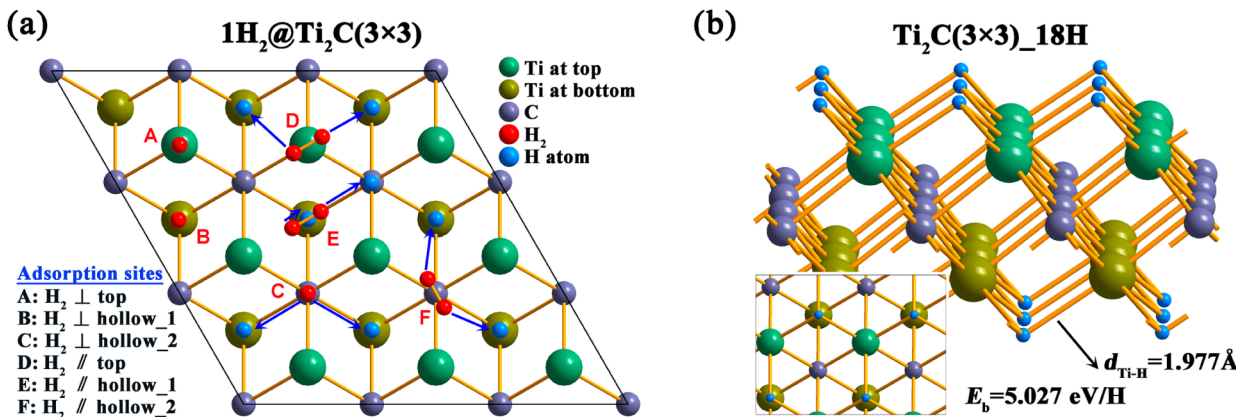


Figure 2. (a) Adsorption of a single hydrogen molecule at different sites of Ti_2C 3×3 supercell. The blue arrows indicate the moving direction of the dissociated H atoms. The black solid line labels out the 3×3 supercell. (b) $\text{Ti}_2\text{C}(3 \times 3)_\text{18H}$ model.

understood that the dissociated H atoms prefer to occupy the hollow_1 site.

We turn our eyes onto the stable A and B adsorption sites in Figure 2a where the H_2 molecules are still intact and perpendicular to the surface. However, if initially the H_2 molecule is put not perpendicular to the A or B sites but is tilted by an angle ($>10^\circ$), the H_2 molecules also dissociate just like the case of parallel to the surface. Therefore, on the basis of the above calculated results, we can presume that the first batch of H_2 molecules arriving onto the clean surface of 2D Ti_2C on the hydrogenation process dissociate into H atoms and then the dissociated H atoms occupy the hollow_1 site. A model, labeled as $\text{Ti}_2\text{C}(3 \times 3)_\text{18H}$ shown in Figure 2b, was constructed to represent this situation. In this model, the H atoms are adsorbed on the hollow_1 sites on both sides of 2D Ti_2C . The calculated binding energy is 5.027 eV per H atom with an H-Ti distance of 1.977 Å. The large binding energy means the interaction of dissociated hydrogen atoms with the Ti_2C surface is of strong chemisorption.

Hydrogen at $\text{Ti}_2\text{C}(3 \times 3)_\text{18H}$ Model. Next, we studied the adsorption of H_2 molecules on the $\text{Ti}_2\text{C}(3 \times 3)_\text{18H}$ structure. Similarly, six models were constructed with one H_2 molecule parallel or perpendicularly above the top, hollow_1 and hollow_2 sites, respectively, as shown in Figure 3. After geometry optimization, the H_2 molecule parallel above the hollow_2 site (labeled as F) relaxes to parallel above the top site (labeled as D). The H_2 molecules for the other five configurations (A, B, C, D, and E; see labels in Figure 3) still keep the initial sites and orientation. For the A, B, C, and E configurations, the calculated binding energies are in the range 30–70 meV, and the H–H bond length increases slightly by 0.01–0.04 Å from the value 0.769 Å of an isolated H_2 . The weak binding energy and the nearly unchanged H–H bond length illuminate the H_2 are physisorbed on the A, B, C, and E sites. An interesting and exciting result is about the configuration that the H_2 is adsorbed parallel on the top site (D in Figure 3). For this configuration, the binding energy is calculated to be 0.237 eV, which falls into the desired range 0.2–0.3 eV. From the binding energy and elongated H–H bond length, we speculated this interaction nature should be of Kubas type, which would be confirmed later by the results of density of states (DOS).

At room temperatures, the hydrogen molecules by physisorption are very little. Therefore, we can presume that under ambient conditions the second batch of H_2 molecules

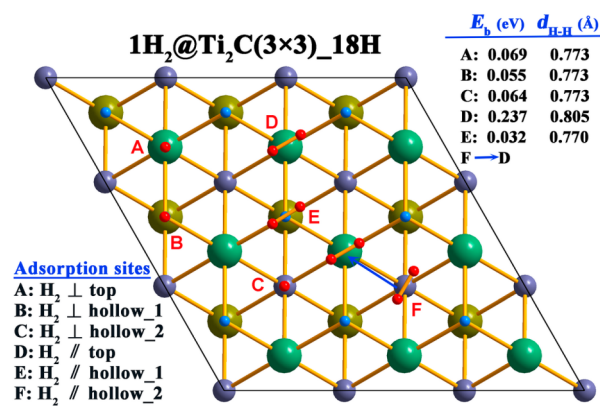


Figure 3. Adsorption of a single hydrogen molecule at different sites of $\text{Ti}_2\text{C}(3 \times 3)_\text{18H}$ model. The calculated binding energies for H_2 at different sites were given. The blue arrow indicates the moving direction of the unstable H_2 molecule. The black solid line labels out the 3×3 supercell. The legend of different atoms is the same to that in Figure 2

arriving on the surface of 2D Ti_2C are adsorbed only parallel on the top site. A model, labeled as $\text{Ti}_2\text{C}(3 \times 3)_\text{18H}_\text{18H}_2$, was constructed as shown in Figure 4a to represent this situation. In this model, onto every top site on both sides was laid one H_2 molecule whose axis is parallel to the surface. The initial orientation of the axes of all the H_2 molecules was set to be the same. After optimization, one-third of the H_2 molecules rotated 60° clockwise around the c axis, one-third of the H_2 molecules rotated 60° counterclockwise around the c axis, and the remaining one-third kept in the original orientation. The optimized structure of $\text{Ti}_2\text{C}(3 \times 3)_\text{18H}_\text{18H}_2$ is shown in Figure 4b. The optimized structure is more symmetrical than the initial structure. The average binding energy for the H_2 molecules by Kubas-type interaction is 0.272 eV per H_2 with an H–H bond length of 0.823 Å.

Hydrogen at $\text{Ti}_2\text{C}(3 \times 3)_\text{18H}_\text{18H}_2$ Model. Now we consider the hydrogen adsorption by physical forces at liquid nitrogen temperatures. At low temperatures, the hydrogen molecules by Kubas-type interaction and the hydrogen atoms by chemisorption are bound tightly to the Ti_2C surfaces. Therefore, the $\text{Ti}_2\text{C}(3 \times 3)_\text{18H}_\text{18H}_2$ model was used as the host material to investigate the physical adsorption of hydrogen molecules. For this model, H_2 molecules have occupied the top sites. Only the hollow_1 and hollow_2 sites could be used to

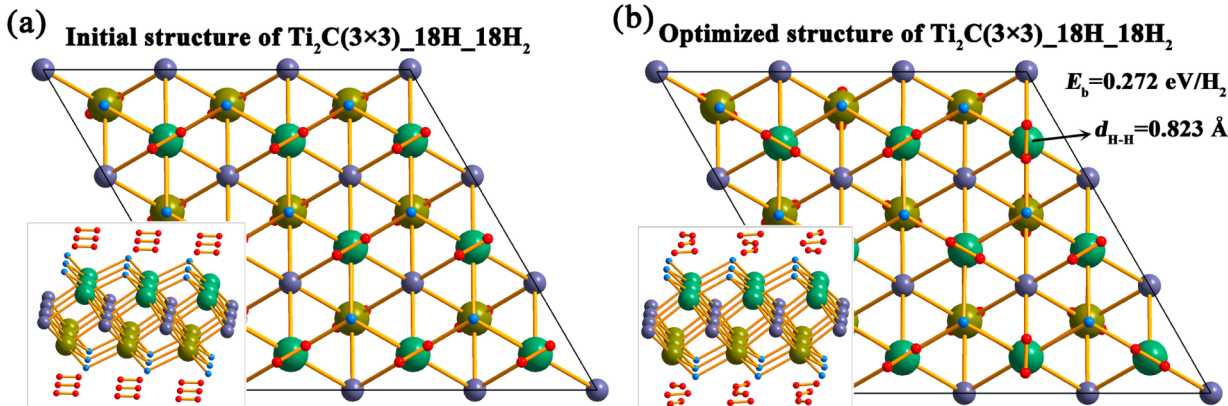


Figure 4. (a) Initial structure of $\text{Ti}_2\text{C}(3\times 3)\text{-}18\text{H-}18\text{H}_2$ model. (b) Optimized structure of $\text{Ti}_2\text{C}(3\times 3)\text{-}18\text{H-}18\text{H}_2$ model. The black solid line labels out the 3×3 supercell. The legend of different atoms is the same to that in Figure 2.

adsorb H_2 molecules. Four configurations, as shown in Figure 5, were constructed in which one H_2 molecule is put parallel or

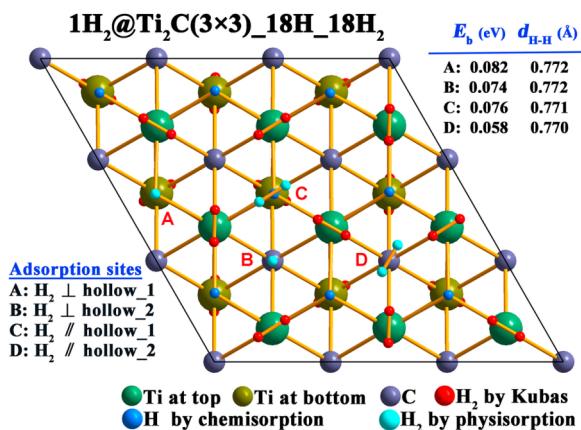


Figure 5. Adsorption of a single hydrogen molecule at different sites of $\text{Ti}_2\text{C}(3\times 3)\text{-}18\text{H-}18\text{H}_2$ model. The calculated binding energies for H_2 at different sites were given. The black solid line labels out the 3×3 supercell.

perpendicularly above the hollow₁ and hollow₂ sites respectively. All four adsorption sites are found to be stable.

The weak binding energies for the four sites mean the nature of physical interaction. For the hollow₁ or hollow₂ site, the binding energies of the parallel and the perpendicular configurations are very close. Thus, at liquid nitrogen temperatures, both the parallel and the perpendicular configurations are possible. Whereas the perpendicular configuration has a little higher binding energy than the corresponding parallel configuration, the two perpendicular configurations were chosen to represent the physisorption of H_2 molecules above the hollow₁ and hollow₂ sites respectively.

A model was constructed to represent this situation, in which every hollow₁ or hollow₂ site on both sides of $\text{Ti}_2\text{C}(3\times 3)\text{-}18\text{H-}18\text{H}_2$ is occupied by one H_2 molecule with its axis perpendicular to the site. After optimization, the H_2 molecules above the hollow₁ site are stable. However, the H_2 molecules above the hollow₂ site depart from the surfaces along the *c*-axis direction. These should arise from the short distance and the resulting repulsion between the H_2 molecules above the hollow₁ site and the neighboring hollow₂ site. A $\text{Ti}_2\text{C}(3\times 3)\text{-}18\text{H-}36\text{H}_2$ model with the H_2 molecules only occupying the hollow₁ site of $\text{Ti}_2\text{C}(3\times 3)\text{-}18\text{H-}18\text{H}_2$ was constructed. Parts a and b of Figure 6 give the top and side views of this model.

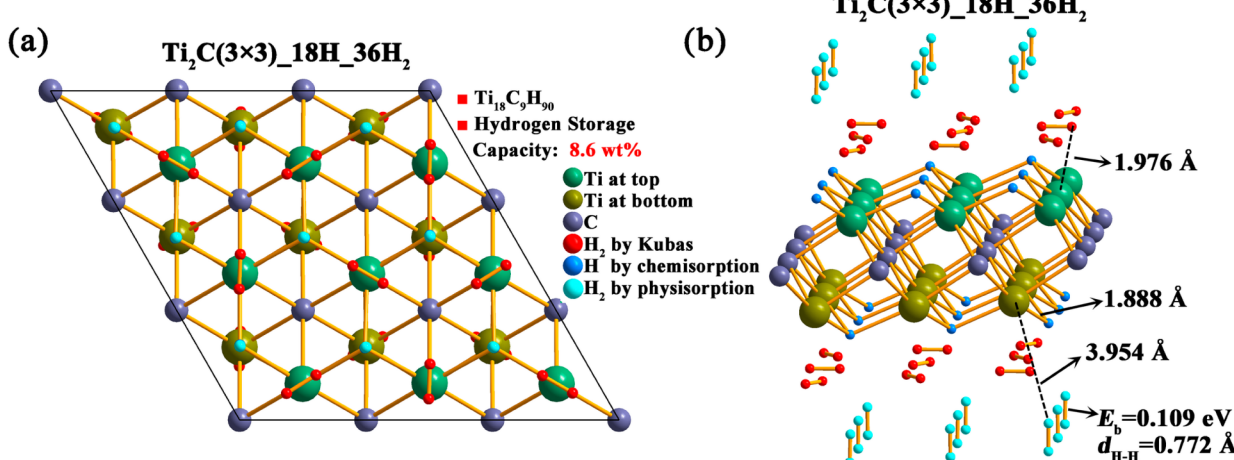


Figure 6. (a) Top views and (b) side views of the $\text{Ti}_2\text{C}(3\times 3)\text{-}18\text{H-}36\text{H}_2$ model that possesses the maximum hydrogen storage capacity. The black solid line labels out the 3×3 supercell.

The average binding energy is calculated to be 0.109 eV per H₂ for these 18 hydrogen molecules above the hollow_1 site.

Maximum Hydrogen Storage Capacity. Now all the possible sites on the Ti₂C surface have been considered to bind hydrogen. In the Ti₂C(3×3)_18H_36H₂ structure, one adsorption site only binds one H₂ molecule. We attempted to attach more H₂ molecules to different adsorption sites. But unfortunately it failed. The new added H₂ molecule directly flies away or pushes the neighboring H₂ molecule off and then occupies its position. Therefore, the Ti₂C(3×3)_18H_36H₂ model possesses the maximum hydrogen storage capacity. In this supercell model, 18 H atoms (1.7 wt %) are bound by strong chemical forces, 36 H atoms (3.4 wt %) are bound in molecule form by weak physical forces, and the remaining 36 H atoms (3.4 wt %) are bound in molecule form by Kubas-type interaction. Under ambient conditions, desorption of chemisorbed hydrogen cannot take place, and physisorbed hydrogens are not easy to bind. Only the hydrogen bound by Kubas-type interaction could be adsorbed and released reversibly under ambient conditions. The reversible capacity of 3.4 wt % is still considerable and significant for practical applications.

Density of States and Mulliken Populations. The Kubas-type interaction between H₂ and transition metals has the following features:^{19,22,45,47} (i) Adsorbed H₂ molecules keep intact and the bond length is elongated approximately 10% from the bond length 0.75 Å of a free H₂ molecule. (ii) The binding energy is between the physisorption and the chemisorption and usually lies in the range 0.2–0.8 eV. (iii) The bond axis of the adsorbed H₂ molecule is not perpendicular to the transition metal. In this paper, the hydrogen molecules adsorbed upon the top sites possess all these features. Hence, we conclude that the binding nature of these hydrogen molecules with Ti₂C should be of the Kubas-type interaction. This Kubas-type interaction is associated with the electron donation of H₂ σ orbitals into the empty d orbitals of a transition metal, and simultaneously the electron back-donation from the filled metal d orbitals into the H₂ σ* antibonding orbitals.^{23,45} Thus the Kubas-type interaction involves the orbital hybridization between the transition metal d orbitals and the H₂ σ orbitals (including bonding and antibonding). Figure 7 gives the partial density of states (PDOS) for the s orbitals of one H₂ molecule above the top site and the 3d orbitals of the underlying Ti atom in the model of Ti₂C(3×3)_18H_36H₂. It can be seen that the Ti 3d orbitals are hybridized with the H₂ σ orbitals in the range −10

to −6 eV. And the peaks from −2 to 0 eV correspond to the hybridization of the Ti 3d with the H₂ σ* orbitals. These hybridizations are very similar to the results obtained by other researches for the adsorption of H₂ on Ti atom.^{19,47}

The approximately 10% elongation of H–H bond length arises from the decrease of bonding-orbital electrons and the increase of antibonding-orbital electrons. If excessive electrons are donated from Ti 3d orbitals to H₂ σ* antibonding orbitals, the H₂ molecule will be unstable and then dissociate. It is the reason that in this study the first H₂ arriving at Ti atom dissociates into H atoms. This phenomenon is also observed in other literatures.^{19,20,48,49} The Mulliken charge population calculations show every dissociated H atom gains 0.33 e totally from the three nearest Ti atoms. This means that every Ti atom donates 0.33 e totally to the three nearest H atoms. Meanwhile, due to the smaller electronegativity of Ti than C, every Ti atom donates about 0.35 e to the three nearest C atoms. Thus when the second H₂ arrives, the Ti atom has no enough charges to destabilize the dihydrogen state. As a result, the second arriving H₂ does not dissociate and locates above the top site in a molecular form. And even, no more charges in the Ti atom can be transferred to bind extra H₂ molecules. It is the reason that one Ti atom can bind 4–6 H₂ molecules in other literatures,^{19,22,47,48} but one Ti atom in the 2D Ti₂C can only bind one H₂ molecule by Kubas-type interaction.

Ab Initio Molecular Dynamic Simulations. From the binding energies results, we speculated that the hydrogen molecules bound by Kubas-type interaction could adsorb and desorb reversibly under ambient conditions. To verify this and ascertain the exact desorption temperature, desorption behaviors of hydrogen on Ti₂C were investigated by ab initio molecular dynamic (MD) simulations using the Nosé algorithm. The simulation temperature was set to be 300 and 400 K. The total simulation time was set to be 1.5 ps with a time step of 1.0 fs. Figure 8 gives the snapshots of the Ti₂C(3×3)_18H_36H₂ model after 1.5 ps molecular dynamic simulations at 300 and 400 K. (Movies 1, 2, 3, and 4 in mpg format for top and side views of desorption processes of hydrogen are available as Web Enhanced Objects.) At both 300 and 400 K, all the H₂ molecules by chemisorption still stay at the initial sites and all the H₂ molecules by physisorption depart from the surfaces. These phenomena can be easily understood from the binding energy results. For the eighteen H₂ molecules by Kubas-type interaction, the results at 300 K are different with those at 400 K. At 400 K, nearly half of the H₂ molecules by Kubas-type interaction depart from the surface. It should be reminded that the simulation system does not reach the balance because the 1.5 ps simulation time is not long enough (however, already quite costly in computation time). Thus the temperature 400 K provides enough energy for the release of the H₂ molecules bound by the Kubas-type interaction. At 300 K, only three H₂ molecules fly away. And an important phenomenon was observed on the simulation process of 300 K. When a released H₂ molecule flies over the region of a vacant top site, the vacant top site can catch and adsorb this H₂ molecule again. Thus at 300 K mostly the top sites should be saturated with H₂ molecules. From the above discussions, the adsorption and desorption of hydrogen by Kubas-type interaction can be accomplished in the narrow temperature range 300–400 K. Therefore, the MD results give clear evidence that 2D Ti₂C is a reversible hydrogen storage material under ambient conditions.

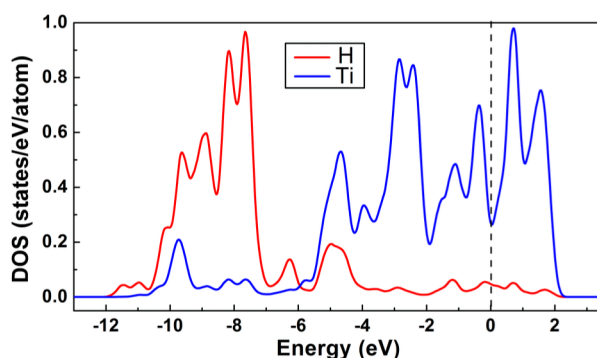


Figure 7. Partial density of states (PDOS) for the s orbitals of one H₂ molecule above the top site and the 3d orbitals of the underlying Ti atom in Ti₂C(3×3)_18H_36H₂ model. The black dash line represents the Fermi level.

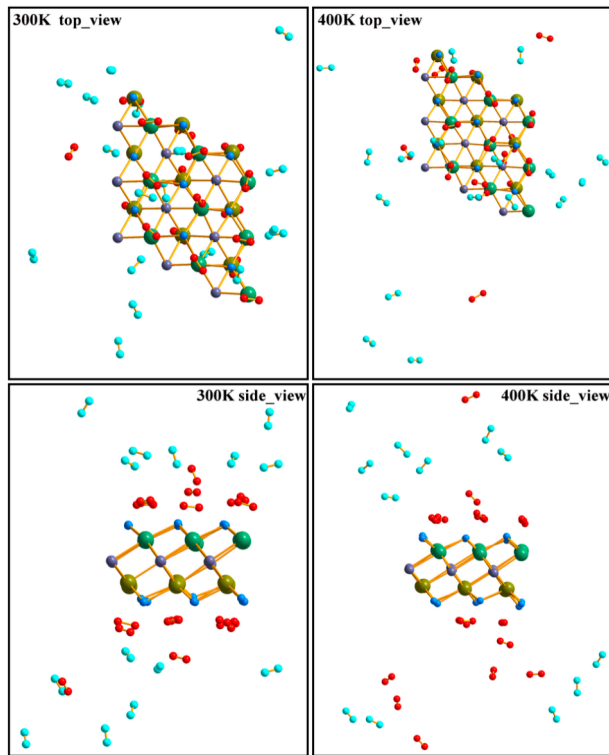


Figure 8. Top and side snapshots of $\text{Ti}_2\text{C}(3\times 3)_\text{18H}_\text{36H}_2$ model after 1.5 ps molecular dynamic simulations at 300 and 400 K. Several hydrogen molecules departing too far from the surfaces were not given. The legend of different atoms is the same to that in Figure 2.

Perspectives of MXene Phases as Hydrogen Storage Materials. An important experimental result should be noted that because MXene phases were made in aqueous hydrofluoric acid, the as-fabricated 2D Ti_2C are chemically terminated with fluorine (F) and/or hydroxyl (OH) groups.^{34,35} The binding interactions are so strong. Thus, although effort has been made,⁴² bare MXene phases with no surface termination have not been prepared. From our point of view, two routes are possible to obtain bare MXene structures: (i) removing the F and OH groups from the synthesized MXenes by chemical or physical methods; (ii) finding a new way to exfoliate parent MAX phases. This is a big challenge and task for materials scientists and chemists. When the writing of this paper came to a close, we realized that the F- or OH-terminated MXene phases may be also a good hydrogen storage material due to the electrostatic interactions between the F (or OH) anions and the adsorbed H_2 . The corresponding calculations are now in progress.

When the A elements are removed from the corresponding MAX family, which includes more than 60 members, theoretically there exist more than 20 MXene phases. These MXene phases have structures and compositions similar to Ti_2C and thus are also expected to be good hydrogen storage materials. To test it, the hydrogen storage properties of 2D Sc_2C and V_2C were calculated in a simple way. We replaced Ti atoms in $\text{Ti}_2\text{C}(3\times 3)_\text{18H}$, $\text{Ti}_2\text{C}(3\times 3)_\text{18H}_\text{18H}_2$, and $\text{Ti}_2\text{C}(3\times 3)_\text{18H}_\text{36H}_2$ models by Sc and V atoms, respectively. The optimized geometry structures (Supporting Information) for hydrogen adsorbed on Sc_2C and V_2C surfaces are similar to those on the Ti_2C surface. The hydrogens are also bound by three modes: physisorption, chemisorption, or Kubas-type interaction. The binding energies for the H_2 on Sc_2C and V_2C

by Kubas-type interaction were calculated to be 0.164 and 0.242 eV per H_2 respectively, which are also suitable. Therefore, the studies in this paper opened the door of a house that contains a series of reversible and high-gravimetric-capacity hydrogen storage materials operated under ambient conditions. And the hydrogen adsorption and desorption behaviors could be adjusted by using different MXene phases as hydrogen storage materials.

CONCLUSIONS

In summary, using first-principles total energy pseudopotential calculations, we systematically investigated the possibility of 2D Ti_2C structure (a representative MXene) as hydrogen storage materials. The calculations show that hydrogen can be adsorbed on different sites on both sides of Ti_2C layered structure. Considering all adsorbed hydrogen molecules and atoms, the maximum hydrogen storage capacity was calculated to be 8.6 wt %, which meets the gravimetric storage capacity target (5.5 wt % by 2015) set by the U.S. DOE. These hydrogen are bound by three modes: chemisorption of the H atom (1.7 wt %), physisorption of the H_2 molecule (3.4 wt %), and Kubas-type binding of the H_2 molecule (3.4 wt %) with calculated binding energies of 5.027, 0.109, and 0.272 eV, respectively. The binding energy of 0.272 eV for the H_2 molecule by Kubas-type interaction just falls into the desired range for a reversible hydrogen storage material under ambient conditions. Ab-initio MD simulations confirmed that the hydrogen molecules bound by Kubas-type interaction can be adsorbed and released reversibly in the temperature range 300–400 K. The different binding energy values for the three modes imply that 2D Ti_2C can store hydrogen at low, room, and high temperatures.

The hydrogen storage properties of Sc_2C and V_2C MXene phases were also evaluated in a simple way. The results are similar to that for Ti_2C and are also fascinating. Therefore, MXene phases including more than 20 members should be a new family of hydrogen storage materials. Experiments are expected to confirm the results of this work. And further experimental and computational investigations should be conducted on other MXene phases. Discovery of MXene phases with better hydrogen storage performances is anticipated in the near future.

ASSOCIATED CONTENT

S Supporting Information

Adsorption geometries and total energies and structural parameters of all the optimized configurations involved in this paper. This material is available free of charge via the Internet at <http://pubs.acs.org>.

W Web-Enhanced Features

Four animations in mpg format are available in the HTML version of the paper.

AUTHOR INFORMATION

Corresponding Authors

*Q. Hu: e-mail, hqk@hpu.edu.cn.

*A. Zhou: e-mail, zhouag@hpu.edu.cn.

Notes

The authors declare no competing financial interest.

ACKNOWLEDGMENTS

This work was supported by National Natural Science Foundation of China (Grant Nos. 51202058, 50802024,

51002045, and 11147167), Program for Innovative Research Team (in Science and Technology) in the University of Henan Province (2012IRTSTHN007), and Innovative Research Team in Henan Polytechnic University (T2013-4). We thank Dr. Zhenhua Chi for revising the English writing of this manuscript.

■ REFERENCES

- (1) Schlapbach, L.; Züttel, A. Hydrogen-Storage Materials for Mobile Applications. *Nature* **2001**, *414*, 353–358.
- (2) Pukazhselvan, D.; Kumar, V.; Singh, S. High Capacity Hydrogen Storage: Basic Aspects, New Developments and Milestones. *Nano Energy* **2012**, *1*, 566–589.
- (3) van den Berg, A. W. C.; Areán, C. O. Materials for Hydrogen Storage: Current Research Trends and Perspectives. *Chem. Commun.* **2008**, 668–681.
- (4) Liu, C.; Li, F.; Ma, L. P.; Cheng, H. M. Advanced Materials for Energy Storage. *Adv. Mater.* **2010**, *22*, E28–E62.
- (5) Hoang, T. K. A.; Antonelli, D. M. Exploiting the Kubas Interaction in the Design of Hydrogen Storage Materials. *Adv. Mater.* **2009**, *21*, 1787–1800.
- (6) Orimo, S.-i.; Nakamori, Y.; Eliseo, J. R.; Züttel, A.; Jensen, C. M. Complex Hydrides for Hydrogen Storage. *Chem. Rev.* **2007**, *107*, 4111–4132.
- (7) Rowsell, J. L.; Yaghi, O. M. Strategies for Hydrogen Storage in Metal–Organic Frameworks. *Angew. Chem., Int. Ed.* **2005**, *44*, 4670–4679.
- (8) Candelaria, S. L.; Shao, Y.; Zhou, W.; Li, X.; Xiao, J.; Zhang, J.-G.; Wang, Y.; Liu, J.; Li, J.; Cao, G. Nanostructured Carbon for Energy Storage and Conversion. *Nano Energy* **2012**, *1*, 195–220.
- (9) Ströbel, R.; Garche, J.; Moseley, P.; Jörissen, L.; Wolf, G. Hydrogen Storage by Carbon Materials. *J. Power Sources* **2006**, *159*, 781–801.
- (10) Pumera, M. Graphene-Based Nanomaterials for Energy Storage. *Energy Environ. Sci.* **2011**, *4*, 668–674.
- (11) Wang, L.; Lee, K.; Sun, Y.-Y.; Lucking, M.; Chen, Z.; Zhao, J.-J.; Zhang, S. B. Graphene Oxide as an Ideal Substrate for Hydrogen Storage. *ACS Nano* **2009**, *3*, 2995–3000.
- (12) Han, S. S.; Kim, H.; Park, N. Effect of Shuttling Catalyst on the Migration of Hydrogen Adatoms: A Strategy for the Facile Hydrogenation of Graphene. *J. Phys. Chem. C* **2011**, *115*, 24696–24701.
- (13) Murray, L. J.; Dincă, M.; Long, J. R. Hydrogen Storage in Metal–Organic Frameworks. *Chem. Soc. Rev.* **2009**, *38*, 1294–1314.
- (14) Suh, M. P.; Park, H. J.; Prasad, T. K.; Lim, D.-W. Hydrogen Storage in Metal–Organic Frameworks. *Chem. Rev.* **2011**, *112*, 782–835.
- (15) Tylianakis, E.; Klontzas, E.; Froudakis, G. E. Multi-Scale Theoretical Investigation of Hydrogen Storage in Covalent Organic Frameworks. *Nanoscale* **2011**, *3*, 856–869.
- (16) Farha, O. K.; Eryazici, I.; Jeong, N. C.; Hauser, B. G.; Wilmer, C. E.; Sarjeant, A. A.; Snurr, R. Q.; Nguyen, S. T.; Yazaydin, A. O.; Hupp, J. T. Metal–Organic Framework Materials with Ultrahigh Surface Areas: Is the Sky the Limit? *J. Am. Chem. Soc.* **2012**, *134*, 15016–15021.
- (17) Eberle, U.; Felderhoff, M.; Schüth, F. Chemical and Physical Solutions for Hydrogen Storage. *Angew. Chem., Int. Ed.* **2009**, *48*, 6608–6630.
- (18) Sigal, A.; Rojas, M.; Leiva, E. Is Hydrogen Storage Possible in Metal-Doped Graphite 2D Systems in Conditions Found on Earth? *Phys. Rev. Lett.* **2011**, *107*, 158701.
- (19) Yildirim, T.; Ciraci, S. Titanium-Decorated Carbon Nanotubes as a Potential High-Capacity Hydrogen Storage Medium. *Phys. Rev. Lett.* **2005**, *94*, 175501.
- (20) Sun, Q.; Wang, Q.; Jena, P.; Kawazoe, Y. Clustering of Ti on a C_{60} Surface and Its Effect on Hydrogen Storage. *J. Am. Chem. Soc.* **2005**, *127*, 14582–14583.
- (21) Sun, Q.; Jena, P.; Wang, Q.; Marquez, M. First-Principles Study of Hydrogen Storage on $Li_{12}C_{60}$. *J. Am. Chem. Soc.* **2006**, *128*, 9741–9745.
- (22) Singh, A. K.; Sadrzadeh, A.; Yakobson, B. I. Metallacboranes: Toward Promising Hydrogen Storage Metal Organic Frameworks. *J. Am. Chem. Soc.* **2010**, *132*, 14126–14129.
- (23) Skipper, C. V.; Hamaed, A.; Antonelli, D. M.; Kaltsoyannis, N. The Kubas Interaction in M (II) ($M = Ti, V, Cr$) Hydrazine-Based Hydrogen Storage Materials: A DFT Study. *Dalton Trans.* **2012**, *41*, 8515–8523.
- (24) Lee, H.; Ihm, J.; Cohen, M. L.; Louie, S. G. Calcium-Decorated Carbon Nanotubes for High-Capacity Hydrogen Storage: First-Principles Calculations. *Phys. Rev. B* **2009**, *80*, 115412.
- (25) Lee, H.; Ihm, J.; Cohen, M. L.; Louie, S. G. Calcium-Decorated Graphene-Based Nanostructures for Hydrogen Storage. *Nano Lett.* **2010**, *10*, 793–798.
- (26) Chan, K. T.; Neaton, J.; Cohen, M. L. First-Principles Study of Metal Adatom Adsorption on Graphene. *Phys. Rev. B* **2008**, *77*, 235430.
- (27) Zhao, Y.; Kim, Y.-H.; Dillon, A.; Heben, M.; Zhang, S. Hydrogen Storage in Novel Organometallic Buckyballs. *Phys. Rev. Lett.* **2005**, *94*, 155504.
- (28) Wu, M.; Gao, Y.; Zhang, Z.; Zeng, X. C. Edge-Decorated Graphene Nanoribbons by Scandium as Hydrogen Storage Media. *Nanoscale* **2012**, *4*, 915–920.
- (29) Kubas, G. J. Dihydrogen Complexes as Prototypes for the Coordination Chemistry of Saturated Molecules. *Proc. Natl. Acad. Sci. U. S. A.* **2007**, *104*, 6901–6907.
- (30) Krasnov, P. O.; Ding, F.; Singh, A. K.; Yakobson, B. I. Clustering of Sc on SWNT and Reduction of Hydrogen Uptake: *Ab-Initio* All-Electron Calculations. *J. Phys. Chem. C* **2007**, *111*, 17977–17980.
- (31) Park, H.-L.; Yi, S.-C.; Chung, Y.-C. Hydrogen Adsorption on Li Metal in Boron-Substituted Graphene: An Ab Initio Approach. *Int. J. Hydrogen Energy* **2010**, *35*, 3583–3587.
- (32) Park, H.-L.; Chung, Y.-C. Metal (Li, Al, Ca and Ti) Absorbed Graphene with Defects for Hydrogen Storage: First-Principles Calculations. *J. Nanosci. Nanotechnol.* **2011**, *11*, 10624–10628.
- (33) http://www.hydrogen.energy.gov/pdfs/review09/program_overview_2009_amr.pdf.
- (34) Naguib, M.; Kurtoglu, M.; Presser, V.; Lu, J.; Niu, J.; Heon, M.; Hultman, L.; Gogotsi, Y.; Barsoum, M. W. Two-Dimensional Nanocrystals Produced by Exfoliation of Ti_3AlC_2 . *Adv. Mater.* **2011**, *23*, 4248–4253.
- (35) Naguib, M.; Mashtalir, O.; Carle, J.; Presser, V.; Lu, J.; Hultman, L.; Gogotsi, Y.; Barsoum, M. W. Two-Dimensional Transition Metal Carbides. *ACS Nano* **2012**, *6*, 1322–1331.
- (36) Barsoum, M. W. The $M_{N+1}AX_N$ Phases: A New Class of Solids: Thermodynamically Stable Nanolaminates. *Prog. Solid State Chem.* **2000**, *28*, 201–281.
- (37) Eklund, P.; Beckers, M.; Jansson, U.; Höglberg, H.; Hultman, L. The $M_{n+1}AX_n$ Phases: Materials Science and Thin-Film Processing. *Thin Solid Films* **2010**, *518*, 1851–1878.
- (38) Kurtoglu, M.; Naguib, M.; Gogotsi, Y.; Barsoum, M. W. First Principles Study of Two-Dimensional Early Transition Metal Carbides. *MRS Commun.* **2012**, *2*, 133–137.
- (39) Shein, I. R.; Ivanovskii, A. L. Graphene-Like Titanium Carbides and Nitrides $Ti_{n+1}C_n$, $Ti_{n+1}N_n$ ($n=1, 2$, and 3) from De-Intercalated MAX Phases: First-Principles Probing of Their Structural, Electronic Properties and Relative Stability. *Comput. Mater. Sci.* **2012**, *65*, 104–114.
- (40) Shein, I. R.; Ivanovskii, A. L. Planar Nano-Block Structures $Ti_{n+1}Al_{0.5}C_n$ and $Ti_{n+1}C_n$ ($n=1$, and 2) from MAX Phases: Structural, Electronic Properties and Relative Stability from First Principles Calculations. *Superlattices Microstruct.* **2012**, *52*, 147–157.
- (41) Tang, Q.; Zhou, Z.; Shen, P. Are MXenes Promising Anode Materials for Li Ion Batteries? Computational Studies on Electronic Properties and Li Storage Capability of Ti_3C_2 and $Ti_3C_2X_2$ ($X = F, OH$) Monolayer. *J. Am. Chem. Soc.* **2012**, *134*, 16909–16916.

- (42) Mashtalir, O.; Naguib, M.; Mochalin, V. N.; Dall'agnese, Y.; Heon, M.; Barsoum, M. W.; Gogotsi, Y. Intercalation and Delamination of Layered Carbides and Carbonitrides. *Nat. Commun.* **2013**, *4*, 1716–1716.
- (43) Naguib, M.; Come, J.; Dyatkin, B.; Presser, V.; Taberna, P.-L.; Simon, P.; Barsoum, M. W.; Gogotsi, Y. MXene: A Promising Transition Metal Carbide Anode for Lithium-Ion Batteries. *Electrochim. Commun.* **2012**, *16*, 61–64.
- (44) Come, J.; Naguib, M.; Rozier, P.; Barsoum, M. W.; Gogotsi, Y.; Taberna, P. L.; Morcrette, M.; Simon, P. A Non-Aqueous Asymmetric Cell with a Ti₂C-Based Two-Dimensional Negative Electrode. *J. Electrochem. Soc.* **2012**, *159*, A1368–A1373.
- (45) Park, N.; Choi, K.; Hwang, J.; Kim, D. W.; Kim, D. O.; Ihm, J. Progress on First-Principles-Based Materials Design for Hydrogen Storage. *Proc. Natl. Acad. Sci. U. S. A.* **2012**, *109*, 19893–19899.
- (46) Clark, S. J.; Segall, M. D.; Pickard, C. J.; Hasnip, P. J.; Probert, M. I.; Refson, K.; Payne, M. C. First Principles Methods Using CASTEP. *Z. Kristallogr.* **2005**, *220*, 567–570.
- (47) Liu, Y.; Ren, L.; He, Y.; Cheng, H.-P. Titanium-Decorated Graphene for High-Capacity Hydrogen Storage Studied by Density Functional Simulations. *J. Phys.: Condens. Matter* **2010**, *22*, 445301.
- (48) Liu, C.-S.; An, H.; Zeng, Z. Titanium-Capped Carbon Chains as Promising New Hydrogen Storage Media. *Phys. Chem. Chem. Phys.* **2011**, *13*, 2323–2327.
- (49) Durgun, E.; Ciraci, S.; Zhou, W.; Yildirim, T. Transition-Metal-Ethylene Complexes as High-Capacity Hydrogen-Storage Media. *Phys. Rev. Lett.* **2006**, *97*, 226102.